ARTICLE
Traditional Medicine Research 2024;9(6):33. https://doi.org/10.53388/TMR20230829002

Efficacy of Juanbi capsule on ameliorating knee osteoarthritis: a network pharmacology and experimental verification-based study

Wen-Bo Huang[1#], Shu-Ya Qin[1#], Jun-Bo Zou[1], Xun Li[2], Wu-Lin Kang[3*], Pu-Wei Yuan[1*]

[1]The First Clinical Medical College of Shaanxi University of Chinese Medicine, Xianyang 712046, China. [2]College of Pharmacy, Shaanxi University of Chinese Medicine, Xianyang 712046, China. [3]Department of Orthopedic, Affiliated Hospital of Shaanxi University of Chinese Medicine, Xianyang 712099, China.

[#]These authors contributed equally to this work and are co-first authors for this paper.
[*]**Correspondence to:** Wu-Lin Kang, Department of Orthopedic, Affiliated Hospital of Shaanxi University of Chinese Medicine, No. 2, Weiyang West Road, Xianyang 712099, China. E-mail: Kangwl1986@126.com; Pu-Wei Yuan, Provincial Key Laboratory of Bone Degenerative Diseases, Shaanxi University of Traditional Chinese Medicine, No. 1 Middle of the Century Avenue, Xianyang 712046, China. E-mail: Spine_surgeon@163.com.

Author contributions
The work was conceived and designed by Kang WL and Huang WB. Laboratory and material support were provided by Yuan PW, while Zou JB offered technical support. The experiment and manuscript were conducted and authored by Huang WB and Qin SY. The data was analyzed by Huang WB. The manuscript was proofread by Li X and Kang WL. The authors declare that all data were generated internally and confirm that no other papers were plagiarized. The manuscript was reviewed by all of the authors.

Competing interests
The authors declare no conflicts of interest.

Acknowledgments
This study received funding from the Basic Research Project of the Education Department of Shaanxi Province (21JC010, 21JP035), the Young and Middle-Aged Scientific Research and Innovation Team of the Shaanxi Provincial Administration of Traditional Chinese Medicine (2022SLRHLJ001), and the 2023 Central Financial Transfer Payment Local Project "Innovation and Improvement of Five Types of Hospital Preparations, Such as Roumudan Granules".

Peer review information
Traditional Medicine Research thanks Qi Shang, Bo Li and other anonymous reviewers for their contribution to the peer review of this paper.

Abbreviations
JBJN, Juanbi capsule; KOA, knee osteoarthritis; TCM, traditional Chinese medicinal; TNF, tumor necrosis factor; IL, interleukin; VEGFA, vascular endothelial growth factor A; BV/TV, bone volume to tissue volume; Tb.Th, trabecular thickness; Tb.N, trabecular number; Tb.Sp, trabecular separation; TCMSP, Traditional Chinese Medicine Systems Pharmacology Database and Analysis Platform.

Citation
Huang WB, Qin SY, Zou JB, Li X, Kang WL, Yuan PW. Efficacy of Juanbi capsule on ameliorating knee osteoarthritis: a network pharmacology and experimental verification-based study. *Tradit Med Res.* 2024;9(6):33. doi: 10.53388/TMR20230829002.

Executive editor: Xi-Yue Liu.
Received: 29 August 2023; **Accepted:** 23 January 2024; **Available online:** 24 January 2024.
© 2024 By Author(s). Published by TMR Publishing Group Limited. This is an open access article under the CC-BY license. (https://creativecommons.org/licenses/by/4.0/)

Abstract
Background: The purpose of the study was to investigate the active ingredients and potential biochemical mechanisms of Juanbi capsule in knee osteoarthritis based on network pharmacology, molecular docking and animal experiments. **Methods**: Chemical components for each drug in the Juanbi capsule were obtained from Traditional Chinese Medicine Systems Pharmacology Database and Analysis Platform, while the target proteins for knee osteoarthritis were retrieved from the Drugbank, GeneCards, and OMIM databases. The study compared information on knee osteoarthritis and the targets of drugs to identify common elements. The data was imported into the STRING platform to generate a protein-protein interaction network diagram. Subsequently, a "component-target" network diagram was created using the screened drug components and target information with Cytoscape software. Common targets were imported into Metascape for GO function and KEGG pathway enrichment analysis. AutoDockTools was utilized to predict the molecular docking of the primary chemical components and core targets. Ultimately, the key targets were validated through animal experiments. **Results**: Juanbi capsule ameliorated Knee osteoarthritis mainly by affecting tumor necrosis factor, interleukin1β, MMP9, PTGS2, VEGFA, TP53, and other cytokines through quercetin, kaempferol, and β-sitosterol. The drug also influenced the AGE-RAGE, interleukin-17, tumor necrosis factor, Relaxin, and NF-κB signaling pathways. The network pharmacology analysis results were further validated in animal experiments. The results indicated that Juanbi capsule could decrease the levels of tumor necrosis factor-α and interleukin-1β in the serum and synovial fluid of knee osteoarthritis rats and also down-regulate the expression levels of MMP9 and PTGS2 proteins in the articular cartilage. **Conclusion**: Juanbi capsule may improve the knee bone microstructure and reduce the expression of inflammatory factors of knee osteoarthritis via multiple targets and multiple signaling pathways.

Keywords: osteoarthritis; inflammation; MMP9/PTGS2; network pharmacology; Juanbi capsule; experimental verification

Highlights

An integrated network pharmacology strategy and experimental evidence were taken to confirm that Juanbi capsule (JBJN) could ameliorate the symptoms of kidney deficiency type osteoarthritis associated with estrogen deficiency. Network analysis indicates that JBJN may ameliorate knee osteoarthritis by primarily regulating the AGE-RAGE, Relaxin, NF-κB signaling pathways, thereby affecting tumor necrosis factor, interleukin 1β, MMP9, PTGS2, vascular endothelial growth factor A, and other cytokines. Animal experiments suggest that JBJN can effectively inhibit the inflammatory response of osteoarthritis and the degradation of cartilage matrix.

Medical history of objective

JBJN, a classical formula of Li's School of Bone Injury in Guanzhong was inspired by Zhang Jiebin's *Jingyue Complete Book: Eight Formations of New Prescriptions* (1624 C.E.) and combined with the clinical experience of Li's School. It is used to treat arthralgia syndrome, which is characterized by pain, swelling, and limitation of movement of the knee or ankle joints. Modern pharmacological research has shown that JBJN is able to regulate the secretion and metabolism of sex hormones, which can enhance the body's immune function and regulate the inflammatory response.

Background

Knee osteoarthritis (KOA) is the predominant form of arthritis, and it is the primary cause of disability and diminished quality of life among middle-aged and elderly individuals [1]. Its pathological changes encompass cartilage degeneration, subchondral bone remodeling, intra-articular osteophyte formation, synovitis, ligament relaxation, contracture, and other related factors [2]. The prevalence of KOA is on the rise due to the aging of society [3]. Currently, the management of KOA primarily centers on the reduction of inflammation, alleviation of pain, and preservation of joint function. In Western medicine, the primary treatment for early-stage KOA is drug therapy, which includes non-steroidal anti-inflammatory drugs, glucosamine, and corticosteroids. Surgical intervention, such as knee replacement, is considered for advanced stages [4]. Given the limitations of Western medicine, including its focus on singular effects, symptom management rather than addressing underlying causes, and potential for serious long-term side effects, there is a critical need to identify a safe and sustainable treatment approach that is both safe and efficacious.

KOA is a prevalent condition in the orthopedic department of traditional Chinese medicine (TCM) and is classified under the "arthralgia syndrome" category of traditional Chinese medicine [5, 6]. The pathogenesis of KOA involves the depletion of essential substances in the liver and kidneys, which results in an inability to meet the nutritional needs of musculoskeletal activities and metabolism in the large joints, such as the knee and ankle. This leads to decreased immunity in these parts, making them vulnerable to the invasion of external pathogenic substances such as wind, cold, dampness, and heat (wind, cold, dampness, and heat are causes of disease resulting from abnormal changes in the natural climate that exceed the body's ability to adapt), which can lead to the blockage of muscles, channels, joints, and the onset of KOA. Therefore, traditional Chinese medicine theory holds that the pathogenesis of KOA is based on the depletion of essential substances in the liver and kidneys, and the invasion of external pathogens is the contributing factor.

The Juanbi capsule (JBJN) (Preparation code: Z20190007, batch number: 2019S00026) is a traditional Chinese medicine preparation produced and used in the Affiliated Hospital of Shaanxi University of Chinese Medicine. This preparation is based on the principle of "tonifying kidney and replenishing qi (qi refers to the various energies of the organs and tissues in the human body)" in the treatment of OA by Professor Li Kanyin, an expert in Chinese medicine doctor specializing in bone injuries, and it is backed by decades of clinical experience. The formulation consists of nine Chinese herbs, which are Yinyanghuo (*Epimedii Folium*), Roucongrong (*Cistanches Herba*), Huangqi (*Astragali Radix*), Danggui (*Angelicae Sinensis Radix*), Gusuibu (*Drynariae Rhizoma*), Shudihuang (*Rehmanniae Radix Praeparata*), Niuxi (*Achyranthis Bidentatae Radix*), Shaoyao (*Paeoniae Radix Alba*), and Gancao (*Glycyrrhizae Radix et Rhizoma*). The function of JBJN is to maintain the liver and kidneys with sufficient intrinsic energy, enhance blood circulation throughout the body, and promote the metabolism of musculoskeletal cells. It is used to alleviate inflammatory symptoms associated with arthralgia syndrome, such as pain, swelling, and limitation of joint movement.

Epidemiological evidence indicates that the prevalence of OA is higher in postmenopausal women and that estrogen deficiency resulting from ovarian dysfunction is a significant factor [7]. According to traditional Chinese medicine, postmenopausal women with estrogen deficiency often exhibit a constitution characterized by low internal energy in the liver and kidney, weakened body immunity, and poor blood circulation. Therefore, the treatment of OA in postmenopausal women should focus on nourishing the intrinsic energy of the liver and kidneys, and improving blood circulation throughout the body. Our previous clinical and basic research has confirmed that the *JBJN* effectively alleviates the pain and swelling symptoms of KOA, particularly in postmenopausal middle-aged and elderly women with arthritis [8, 9]. Therefore, we established a new method of inducing estrogen deficiency-induced OA by ovariectomizing and Hulth to examine the therapeutic effects of JBJN on the development of KOA in a rat model with kidney deficiency.

In order to conduct a comprehensive investigation of JBJN, it is essential to elucidate its mechanism of action. In this study, network pharmacology was used to investigate the active ingredients, targets, and mechanisms of JBJN in the treatment of KOA. Subsequent to this, experiments involving animals were carried out to further confirm the effectiveness of the treatment and to offer valuable insights for clinical application and further research of JBJN.

Materials and methods

Collection of chemical components and prediction of JBJN

The Traditional Chinese Medicine Systems Pharmacology Database and Analysis Platform (TCMSP) is a digital information platform that disseminates the primary constituents of traditional Chinese medicine [10]. The active compounds in JBJN were retrieved from the TCMSP database for the purposes of this study. Compounds with an oral bioavailability of 30% or higher and a drug-likeness score of 0.18 or greater are considered to exhibit enhanced pharmacological effects and are thus selected for further analysis as potential active compounds. The compounds searched under these conditions were the candidate components, after which the target proteins corresponding to the candidate components were identified and categorized. Utilizing the UniProt data platform (https://www.uniprot.org/), the species was set to "Homo sapiens", following which the target proteins of JBJN were inputted, and the corresponding gene names for each protein were searched, thereby revealing the target proteins of JBJN.

KOA target prediction

By searching Drugbank (https://www.drugbank.ca/), GeneCards (https://www.genecards.org/), and OMIM database (https://www.omim.org), the keyword "knee osteoarthritis" and the species "Homo sapiens" were used to screen for KOA targets.

Construction of a chemical component-target network of JBJN

Cytoscape 3.9.1 software was utilized to construct the chemical component-target network of JBJN in section 2.1. Based on the Degree of connectivity, Betweenness, and Closeness, the primary chemical components in JBJN were identified.

Construction of the PPI network

Using R software, we aimed to identify the common target proteins in sections 2.1 and 2.2, which may represent genes targeted by JBJN during KOA, and create a Venn diagram. Next, we constructed the protein-protein interaction (PPI) network model using the STRING database (https://www.string-db.org/). Cytoscape 3.9.1 software was utilized to build and analyze the PPI network map using the files obtained from the STRING database in order to identify the core targets of JBJN that affect KOA.

GO and KEGG pathway enrichment analysis

KOA was inputted into the Metascape data platform (https://metascape.org/) for annotation, visualization, and analysis of GO and KEGG pathway enrichment to predict molecular functions, biological pathways, and other related factors of JBJN in the treatment of KOA. The results of the analyses are mainly presented as p-values, where p-values are arranged in ascending order. The p-values are negatively correlated with enrichment degree, where the smaller the p-value, the higher the enrichment degree of this pathway and the greater its importance in the process of treating KOA with JBJN.

Molecular docking

The 3D structures of target proteins and chemical components were downloaded from the RCSB PDB database (https://www1.rcsb.org) and the TCMSP database. AutoDock Tools software was used to perform molecular docking for the main chemical components obtained from section 2.3 and the core targets screened in section 2.4.

Animal selection and ethical statement

Twenty-four 8-week-old female Sprague-Dawley rats, weighing 200 ± 20 g, were obtained from the Experimental Animal Center of Shaanxi University of Traditional Chinese Medicine, with license number SCXK (Shaan) 2021-001. After completing quarantine, the animals were housed in the SPF animal room at the Animal Experimental Center of Shaanxi University of Traditional Chinese Medicine, where they received daily food and water provided by the center. This experiment has been reviewed by the Animal Ethics Committee of Shaanxi University of Traditional Chinese Medicine (Ethics number: SUCMDL20220621002). The animal experiment was performed in line with the Guidelines for the Management and Use of Laboratory Animals by the Chinese National Institutes of Health. Finally, criteria established for euthanizing rat were performed according to ARRIVE 2.0 guidelines rigorously.

Main reagents and instruments

The extract of JBJN, prepared by the Preparation Center of Affiliated Hospital of the Shaanxi University of Chinese Medicine (Xianyang, China), was used as the experimental drug. Rat tumor necrosis factor (TNF)-α and interleukin (IL)-1β ELISA kit were produced by Boster (Wuhan, China, batch number 11518103103 and 24018991031). Anti-MMP9 Antibody was produced by Abcam (Cambridge, UK, batch number: 1006593-1). Anti-PTGS2 antibody was produced by Proteintech (Wuhan, China, batch number: 00100441). Anti-β-actin antibody was produced by Boorson (Beijing, China, batch number: AH11286487), BCA protein concentration determination kit was produced by Boster (Wuhan, China, batch number: 18D17B46), SDS-PAGE gel rapid preparation kit was produced by Xavier (Wuhan, China, batch number: CR2302001).

Model establishing, grouping, and treating

The rats were randomly divided into three groups: a normal control group (Control), a KOA model control group (Model), and a JBJN treatment group, with 8 rats in each group. The Hulth method and bilateral ovariectomy were used to induce KOA rat models with kidney deficiency in the Model and JBJN groups [11, 12]. After 6 weeks, 3 rats were randomly selected from the model group and the JBJN group for micro-CT scanning of the knee joint. The joint space on the model side was narrower than that on the healthy side, and subchondral sclerosis or osteophyte formation indicated the successful establishment of the KOA model. After successfully establishing the model, the rats in the JBJN group were administered JBJN by gavage, while the rats in the Control and Model groups were given an equivalent amount of distilled water by gavage. The three groups were treated for 6 weeks.

The clinically administered oral dose of JBJN for humans (70 kg) was 127 g/d, and according to the human-rat body surface area dose conversion method, the equivalent dose of rats was 6.3 times that of humans. Thus, a rat was given equivalent doses of crude drug of JBJN of 11.43 g/kg daily.

Micro-CT scan

Three rats from each group were randomly selected to take the intact left knee joint, and Skyscan1276 was used for scanning with micro-CT equipment (Bruker, Belgium). After fixing the samples, the scanning voltage was set to 60 kV, and the scanning current was set to 200 μA. The knee joint was scanned along the long axis of the femur using a scanning thickness of 10 μm, a filter of AL0.5 mm, and an exposure time of 550 ms to obtain continuous plane micro-CT images. After scanning, 3D reconstruction processing software NRecon and Data Viewer were used to reconstruct and select, and CT Analyzer was used to quantitatively analyze the cartilage and subchondral bone areas in the same position in the image. The microstructure parameters of tibia trabecular bone were analyzed, including bone volume to tissue volume (BV/TV), trabecular thickness (Tb.Th), trabecular number (Tb.N), and trabecular separation (Tb.Sp).

ELISA detection

After intraperitoneal anesthesia with 1% sodium pentobarbital (4 mL/kg), blood samples were collected from the abdominal aorta and allowed to stand at 4 ˚C for two hours before centrifugation at 3500 rpm for fifteen minutes. Knee punctures were performed, and a sterile medical syringe was used to inject 1 mL of sterile PBS solution into the knee joint. Subsequently, the knee joint was exercised ten times, followed by the slow extraction of the joint fluid. The extracted fluid was then allowed to stand at 4 ˚C for one hour before being centrifuged at 3,500 rpm for twenty minutes. The concentrations of TNF-α and IL-1β in both serum and joint fluid were determined using an ELISA kit following the provided instructions.

Western blot detection

The articular cartilage samples from each group were frozen in liquid nitrogen for ten minutes. Then, 500 μL of RIPA and PMSF (in a 100:1 ratio) were added, and the samples were ground in a frozen grinder (−49 ˚C). After grinding, the cartilage was placed on ice for fifteen minutes to allow the protein to fully dissolve. Subsequently, the homogenate was centrifuged to obtain a solution of total proteins.

Protein samples were prepared by adding a loading buffer to ensure consistent protein concentrations of 50 μg/10 μL for each group. The protein samples were separated using 10% SDS-PAGE and subsequently transferred onto the PVDF membrane. The membrane was then blocked with 5% skim milk for 2 hours, followed by overnight incubation with primary antibodies (MMP9 at a dilution of 1:2,000, PTGS2 at a dilution of 1:1,500) at 4 ˚C. After incubating with secondary antibodies for 90 minutes at room temperature, the films were developed using ECL chemiluminescence solution and then scanned using ImageJ software following exposure. β-actin served as an internal control.

Statistical analysis

All statistical analyses were conducted using the SPSS 26.0 software. The data were presented as mean ± standard deviation ($\bar{x} \pm s$). One-way ANOVA with Tukey's post hoc test was used for comparing multiple groups, a significance level of $P < 0.05$ was employed as the threshold to ascertain statistical significance.

Results

Screening of chemical component

Traditional Medicine Research 2024;9(6):33. https://doi.org/10.53388/TMR20230829002

The TCMSP database was utilized to search for 167 chemical components of JBJN, including 23 from *Epimedii Folium*, 6 from *Cistanches Herba*, 17 from *Astragali Radix*, 2 from *Angelicae Sinensis Radix*, 15 from *Drynariae Rhizoma*, 2 from *Rehmanniae Radix Praeparata*, 17 from *Achyranthis Bidentatae Radix*, 7 from *Paeoniae Radix Alba*, and 88 from *Glycyrrhizae Radix et Rhizoma*. Additionally, there are 13 common chemical components between each drug (Table 1).

Table 1 Basic information of main active compounds in JBJN

Mol ID	Label	Chemical Component	OB (%)	DL	Source
MOL000622	YYH18	Magnograndiolide	63.71	0.19	*Epimedii Folium*
MOL004367	YYH6	Olivil	62.23	0.41	
MOL004388	YYH12	6-hydroxy-11,12-dimethoxy-2,2-dimethyl-1,8-dioxo-2,3,4,8-tetrahydro-1H- isochromeno[3,4-h]isoquinolin-2-ium	60.64	0.66	
MOL004382	YYH9	Yin	56.96	0.77	
MOL004396	YYH15	1,2-bis(4-hydroxy-3-methoxyphenyl)propan-1,3-diol	52.31	0.22	
MOL005320	RCR1	arachidonate	45.57	0.2	*Cistanches Herba*
MOL005384	RCR2	suchilactone	57.52	0.56	
MOL007563	RCR3	Yangambin	57.53	0.81	
MOL008871	RCR4	Marckine	37.05	0.69	
MOL000378	HQ9	7-O-methylisomucronulatol	74.69	0.3	*Astragali Radix*
MOL000433	HQ8	FA	68.96	0.71	
MOL000380	HQ7	(6aR,11aR)-9,10-dimethoxy-6a,11a-dihydro-6H-benzofurano[3,2-c]chromen-3-ol	64.26	0.42	
MOL000371	HQ6	3,9-di-O-methylnissolin	53.74	0.48	
MOL000439	HQ12	isomucronulatol-7,2'-di-O-glucosiole	49.28	0.62	
MOL005190	GSB5	eriodictyol	71.79	0.24	*Drynariae Rhizoma*
MOL009078	GSB9	davallioside A_qt	62.65	0.51	
MOL000569	GSB6	digallate	61.85	0.26	
MOL000492	GSB4	(+)-catechin	54.83	0.24	
MOL001978	GSB2	Aureusidin	53.42	0.24	
MOL000785	NX12	palmatine	64.6	0.65	*Achyranthis Bidentatae Radix*
MOL002897	NX9	epiberberine	43.09	0.78	
MOL001006	NX1	poriferasta-7,22E-dien-3beta-ol	42.98	0.76	
MOL004355	NX11	Spinasterol	42.98	0.76	
MOL002776	NX8	Baicalin	40.12	0.75	
MOL001918	BS1	paeoniflorgenone	87.59	0.37	*Paeoniae Radix Alba*
MOL001919	BS2	(3S,5R,8R,9R,10S,14S)-3,17-dihydroxy-4,4,8,10,14-pentamethyl-2,3,5,6,7,9-hexahydro-1H-cyclopenta[a]phenanthrene-15,	43.56	0.53	
MOL001924	BS3	paeoniflorin	53.87	0.79	
MOL002311	GC2	Glycyrol	90.78	0.67	*Glycyrrhizae Radix et Rhizoma*
MOL004990	GC64	7,2',4'-trihydroxy − 5-methoxy-3 − arylcoumarin	83.71	0.27	
MOL004904	GC38	licopyranocoumarin	80.36	0.65	
MOL004891	GC35	shinpterocarpin	80.3	0.73	
MOL005017	GC76	Phaseol	78.77	0.58	
MOL000417	A1	Calycosin	47.75	0.24	*Astragali Radix, Glycyrrhizae Radix et Rhizoma*
MOL000354	A2	isorhamnetin	49.6	0.31	
MOL000239	A3	Jaranol	50.83	0.29	
MOL000392	A4	formononetin	69.67	0.21	
MOL001792	A5	DFV	32.76	0.18	*Epimedii Folium, Glycyrrhizae Radix et Rhizoma*
MOL000006	A6	luteolin	36.16	0.25	*Epimedii Folium, Drynariae Rhizoma*
MOL004328	A7	naringenin	59.29	0.21	*Drynariae Rhizoma, Glycyrrhizae Radix et Rhizoma*
MOL000211	B1	Mairin	55.38	0.78	*Astragali Radix, Paeoniae Radix Alba, Glycyrrhizae Radix et Rhizoma*
MOL000449	C1	Stigmasterol	43.83	0.76	*Angelicae Sinensis Radix, Drynariae Rhizoma, Achyranthis Bidentatae Radix, Rehmanniae Radix Praeparata*
MOL000359	C2	sitosterol	36.91	0.75	*Epimedii Folium, Rehmanniae Radix Praeparata, Paeoniae Radix Alba, Glycyrrhizae Radix et Rhizoma*
MOL000098	D1	quercetin	46.43	0.28	*Astragali Radix, Epimedii Folium, Cistanches Herba, Achyranthis Bidentatae Radix, Glycyrrhizae Radix et Rhizoma*
MOL000358	D2	beta-sitosterol	36.91	0.75	*Angelicae Sinensis Radix, Cistanches Herba, Drynariae Rhizoma, Achyranthis Bidentatae Radix, Paeoniae Radix Alba*
MOL000422	E1	kaempferol	41.88	0.24	*Astragali Radix, Epimedii Folium, Drynariae Rhizoma, Achyranthis Bidentatae Radix, Paeoniae Radix Alba, Glycyrrhizae Radix et Rhizoma*

Due to the large number of chemical compounds of drug, only the top 5 compounds of OB are listed in the table. JBJN, Juanbi capsule; OB, oral bioavailability; DL, drug-like properties.

Traditional Medicine Research 2024;9(6):33. https://doi.org/10.53388/TMR20230829002

Construction and analysis of chemical component-target network

The DrugBank and UniProt databases were utilized to search for 315 target proteins associated with the chemical components of JBJN. Subsequently, we obtained information about the drug composition, chemical components, and their respective relationships with targets. Using Cytoscape 3.9.1 software, a network illustrating the interactions between JBJN chemical components and targets was constructed. This network consisted of a total of 475 nodes, which included 9 drug nodes, 167 active compound nodes, and 315 target nodes, all connected by a total of 4,135 edges (Figure 1).

Figure 1 shows that each chemical component interacts with multiple targets while each target corresponds to multiple chemical components simultaneously or independently affiliated with each traditional Chinese medicine. These findings indicate that JBJN exerts its effects on KOA through multiple components, targets, and pathways. Notably, quercetin, kaempferol, beta-sitosterol, Stigmasterol, and luteolin emerged as the main active compounds based on their higher Degree values.

Target prediction and mutual PPI network construction

The DrugBank, GeneCards, and OMIM databases were utilized to search for 363 KOA targets. Subsequently, drug and disease targets were incorporated into the R software, resulting in 49 overlapping targets (Figure 2).

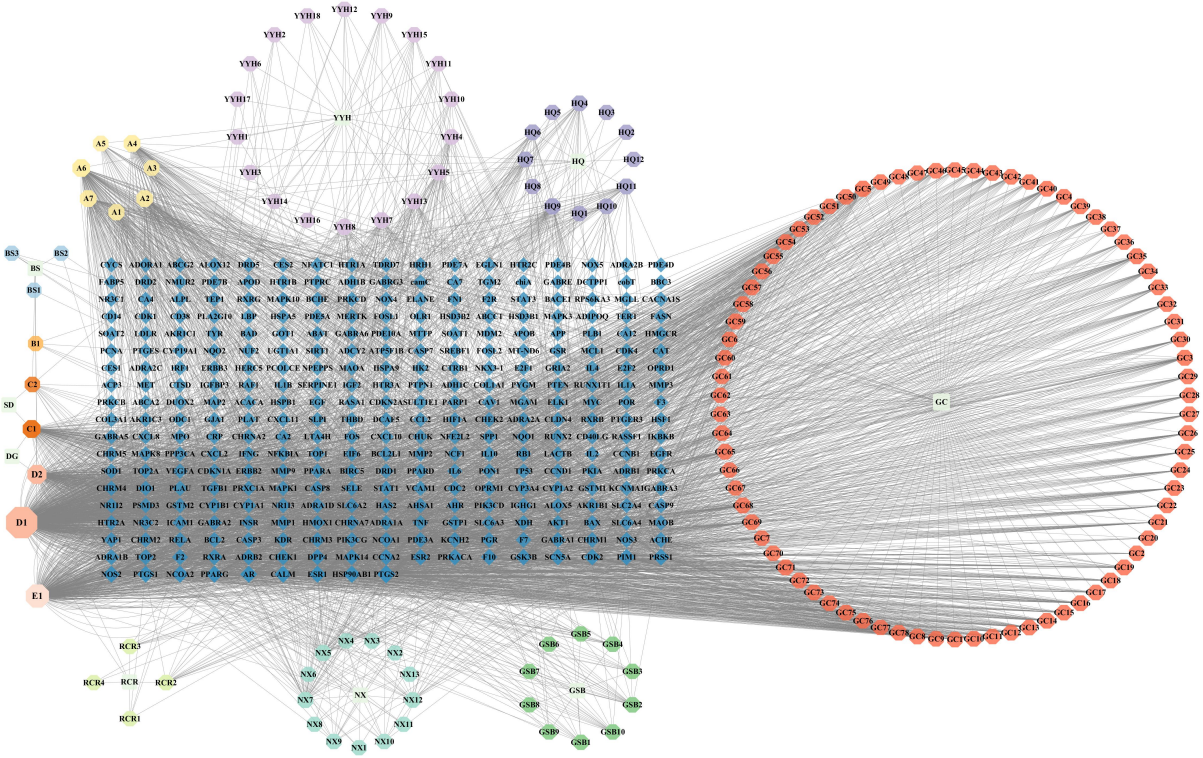

Figure 1 Compounds of JBJN-chemical component-target network. The blue square part in the figure is candidate targets, and the surrounding circular part is chemical components of the JBJN compound. The darker the color and the larger the shape, the higher the degree value, and each edge represents the relationship between the compound and the target. JBJN, Juanbi capsule.

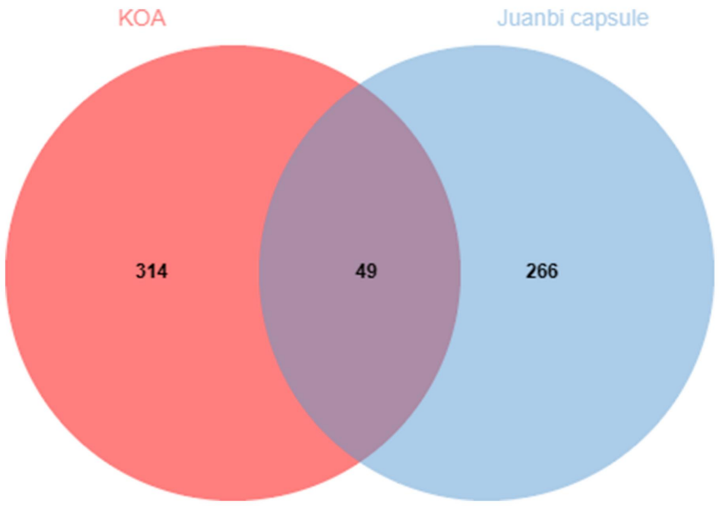

Figure 2 The overlapping targets of JBJN in KOA treatment. The Venn diagram demonstrates the number of intersected and specific targets between JBJN and KOA. JBJN, Juanbi capsule; KOA, knee osteoarthritis.

Traditional Medicine Research 2024;9(6):33. https://doi.org/10.53388/TMR20230829002

Overlapping targets of JBJN and KOA were retrieved from the STRING databases and imported into the Cytoscape software platform to generate the PPI network diagram (Figure 3). This network comprises a total of 48 nodes and 603 edges. The nodes represent the target proteins, and the edges represent the interactions between different target proteins. According to Figure 3, TNF, IL6, IL1B, MMP9, PTGS2, VEGFA, TP53, and other target proteins are the central targets in this network.

Enrichment analysis of overlapping target by GO and KEGG pathway

GO enrichment analysis of the overlapping targets between JBJN and KOA was performed using the Metascape data platform. Through analysis, a total of 1,072 GO items representing potential targets of JBJN were obtained. Among them, 975 items were related to biological processes, 72 items were related to molecular functions, and 25 items were related to cellular components. The top 10 items in biological processes, cellular components, and MF were selected to create the bubble diagram (Figure 4A). The biological processes Involved in the treatment of KOA by JBJN mainly include regulation

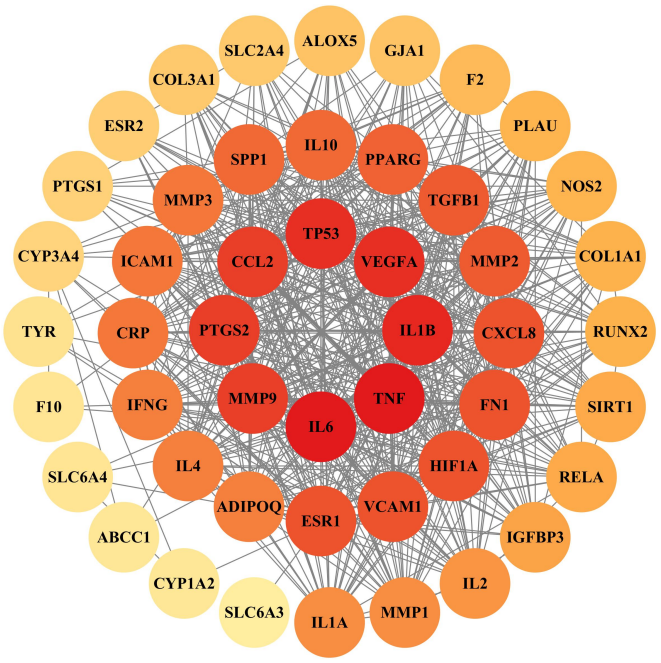

Figure 3 PPI network diagram of overlapping targets. Critical targets of JBJN in treating KOA were screened by degree values, in which the darker color and the closer nodes to the center have higher degree values. JBJN, Juanbi capsule; KOA, knee osteoarthritis; TNF, tumor necrosis factor; IL, interleukin.

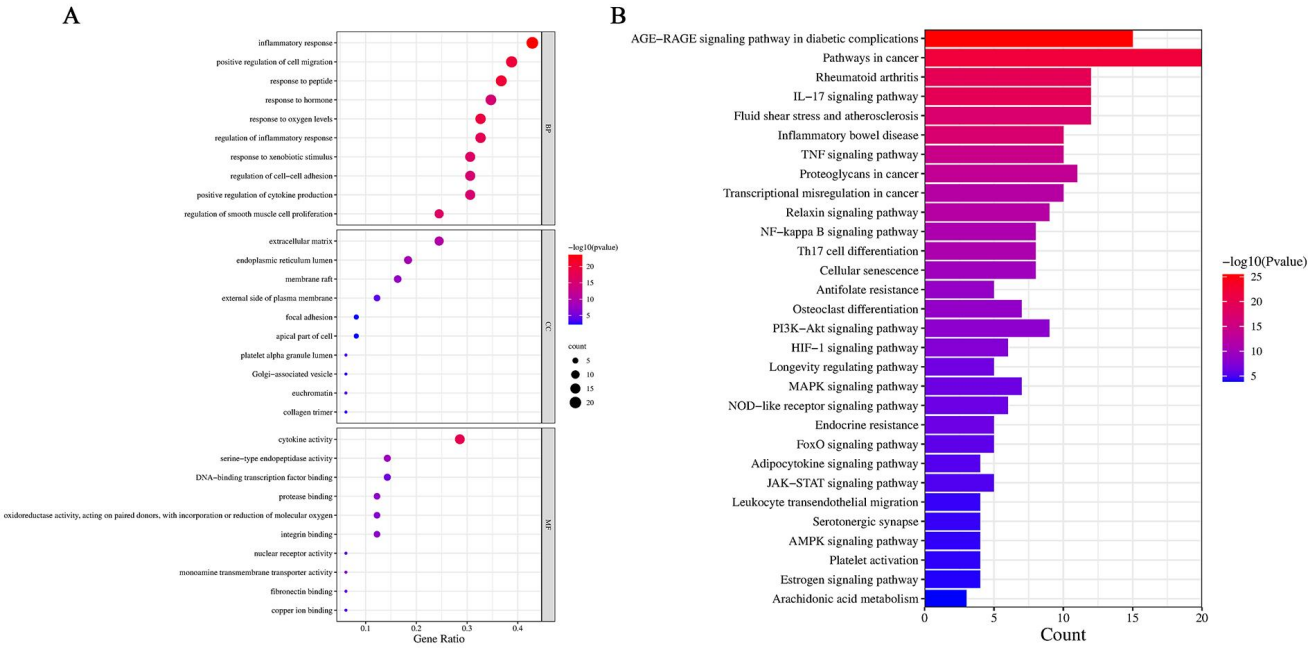

Figure 4 Enriched Go and KEGG signaling pathways of overlapping targets. (A) The Bubble chart shows the top ten in the BP, CC, and MF categories in the GO enrichment analysis. (B) The Bar graph of the top 30 pathways extracted by KEGG analysis. BP, biological process; CC, cell component; MF, molecular function.

of inflammatory response, cell migration, signal peptide activity, metabolism of reactive oxygen species, hormonal stress, and response to xenobiotic stimulation. The cellular components include the extracellular matrix, endoplasmic reticulum lumen, membrane raft, and outer membrane of the plasma membrane. Molecular functions include cytokine activity, serine endopeptidase activity, protease binding, integrin binding, oxidoreductase activity, and DNA binding transcription factor binding.

KEGG pathways were identified using the Metascape data platform, and signaling pathways that significantly influence the treatment of KOA by JBJN were analyzed. A total of 107 KEGG pathways with significant enrichment of potential targets of JBJN were obtained ($P < 0.05$). According to the significance arrangement, the top 30 items were selected and depicted in a bar chart (Figure 4B). The treatment of KOA by JBJN mainly involves targeting the cancer pathway, AGE-RAGE signaling pathway, IL-17 signaling pathway, TNF signaling pathway, Relaxin signaling pathway, NF-κB signaling pathway, Th17 cell differentiation, PI3K-Akt signaling pathway, HIF-1 signaling pathway, MAPK signaling pathway, and others.

Molecular docking

The primary chemical components (quercetin, kaempferol, β-sitosterol) identified in section 3.2 were docked with key targets (TNF, IL1B, MMP9, PTGS2, VEGFA, TP53) identified in section 3.3, and the results of the docking are presented in Table 2. The average affinity between each molecule was −6.942 kcal/mol, which was lower than −5 kcal/mol, indicating that the primary chemical components of JBJN exhibited a strong binding ability to the target protein [13]. The results indicate that all the chemical components of JBJN penetrated deeply into the active site and formed a relatively stable conformation with the target receptor protein through hydrogen bonding. Some molecular docking binding modes are shown in Figure 5.

Assessment of the KOA rat model

The 2D images obtained from the micro-CT revealed that the knee

Table 2 Results of molecular docking

Chemical component	Target protein	PDB ID	Affinity (kcal/mol)
MOL000098	TNF	6X81	−6.95
MOL000358	TNF	6X81	−6.51
MOL000422	TNF	6X81	−7.78
MOL000098	IL1B	6Y8M	−6.42
MOL000358	IL1B	6Y8M	−5.63
MOL000422	IL1B	6Y8M	−7.59
MOL000098	MMP9	5TH6	−7.52
MOL000358	MMP9	5TH6	−7.34
MOL000422	MMP9	5TH6	−8.71
MOL000098	PTGS2	4RRW	−5.87
MOL000358	PTGS2	4RRW	−7.21
MOL000422	PTGS2	4RRW	−5.89
MOL000098	VEGFA	6ZCD	−7.1
MOL000358	VEGFA	6ZCD	−6.4
MOL000422	VEGFA	6ZCD	−9.37
MOL000098	TP53	8D6C	−5.36
MOL000358	TP53	8D6C	−6.1
MOL000422	TP53	8D6C	−7.21

PDB ID, Protein Data Bank identification; TNF, tumor necrosis factor; IL, interleukin.

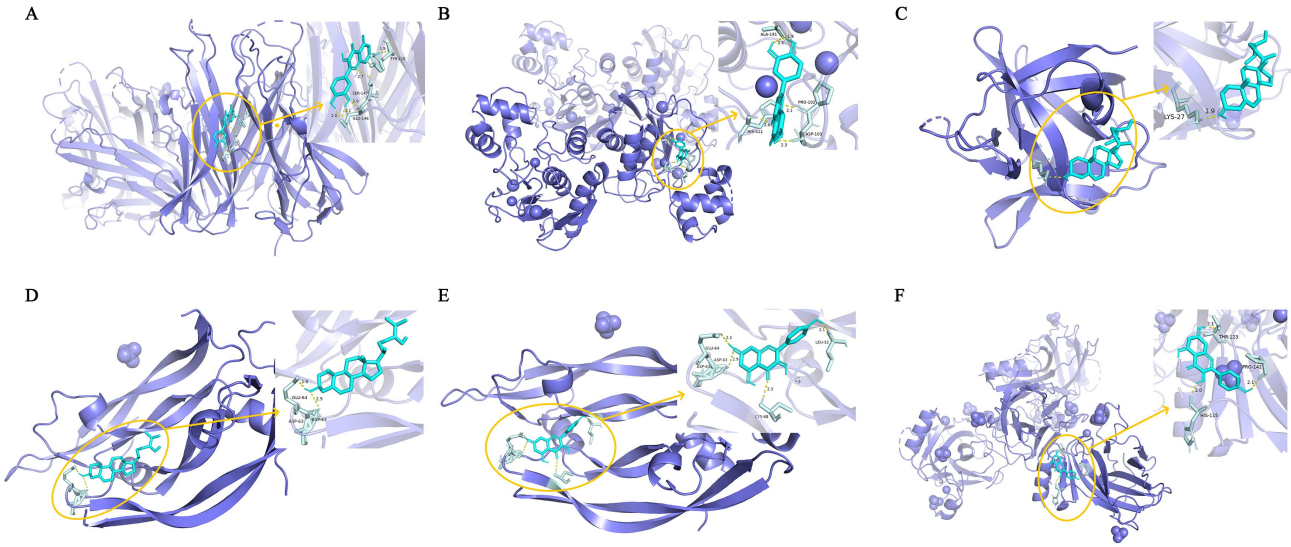

Figure 5 Molecular docking pattern diagram of critical core protein targets. The yellow circles represent the docking states between small molecule compounds and macromolecular proteins, and the short yellow lines represent hydrogen bonds. (A, B) The docking status of quercetin with TNF and MMP9 respectively. (C, D) The docking status of kaempferol with IL1B and VEGFA, respectively. (E, F) The docking status of β-sitosterol with VEGFA and TP53 respectively. IL, interleukin; VEGFA, vascular endothelial growth factor A; TNF, tumor necrosis factor.

joint surface of rats in the normal control group was relatively smooth, with a normal joint space and no observed osteophytes. In contrast, the joint surface of the model control group 6 weeks after the operation appeared uneven, with hardened subchondral bone and the formation of osteophytes (Figure 6).

Effect of JBJN on knee joint in KOA rats with micro-CT

Micro-CT analysis of the subchondral bone structure revealed that, compared to the normal control group, the model control group exhibited a significantly narrower medial joint space and disordered microstructure of trabecular bone in the subchondral region, indicating the successful establishment of the animal model. The treatment with JBJN demonstrated an improvement in both the joint space and the trabecular meshwork structure of the subchondral bone (Figure 7A).

To evaluate changes in the subchondral bone, the medial tibial

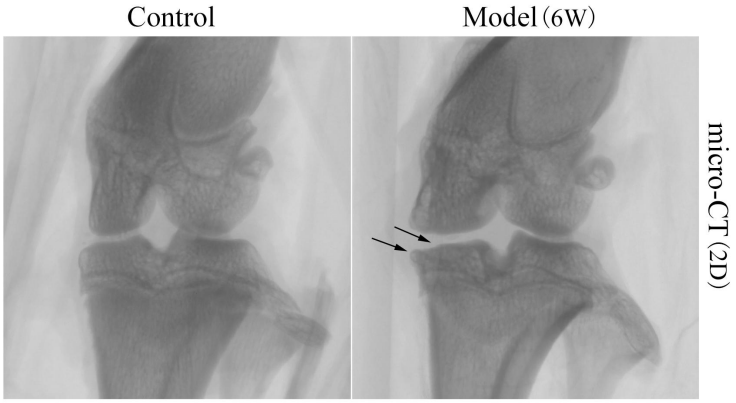

Figure 6 Microstructural changes in the knee articular surface in KOA model rats. 2D imaging of the structure of the subchondral bone of the tibia. The black arrows indicate the damaged region of the articular surface. KOA, knee osteoarthritis.

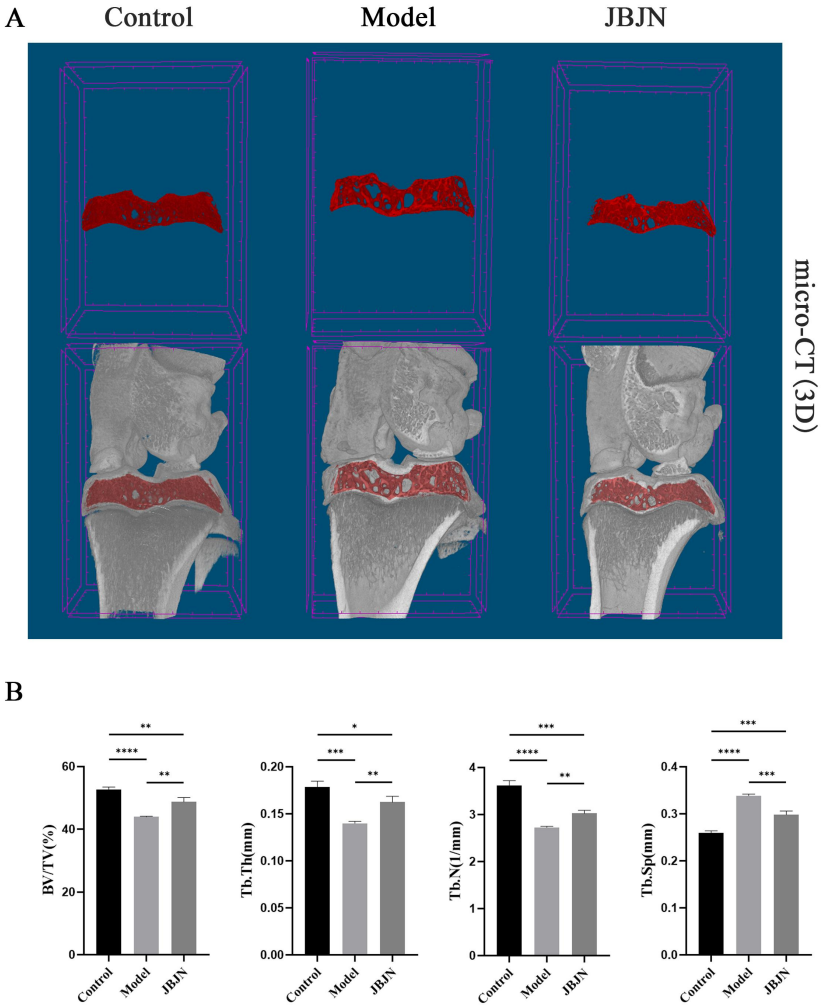

Figure 7 JBJN protects against bone microstructure damage caused by KOA. (A) Micro-CT section 3D images of the coronal tibia in each group. (B) Quantitative analysis of BV/TV, Tb.Th, Tb.N, Tb.Sp ($\bar{x} \pm s$, $n = 3$). One-way ANOVA (with Tukey's post-hoc test) was used for the statistical analysis. The significance levels were denoted as $^{*}P < 0.05$, $^{**}P < 0.01$, $^{***}P < 0.001$, and $^{****}P < 0.0001$. JBJN, Juanbi capsule; KOA, knee osteoarthritis; BV/TV, bone volume to tissue volume; Tb.Th, trabecular thickness; Tb.N, trabecular number; Tb.Sp, trabecular separation; ANOVA, analysis of variance.

plateau was quantitatively analyzed in each group. Bone volume to tissue volume, trabecular thickness, trabecular number, and trabecular separation revealed bone microstructure damage in the model control group. These indicators showed improvement with JBJN treatment (Figure 7B).

Effect of JBJN on the expression of inflammatory factors in KOA rats

The analysis of inflammatory factor levels in the serum showed that the expression levels of TNF-α and IL-1β were significantly lower in the JBJN group compared to the model control group (Figure 8A). Subsequently, the changes in expression of TNF-α and IL-1β in the joint fluid were detected to further confirm that the levels in the JBJN group were also significantly lower than those in the model control group (Figure 8B).

Effect of JBJN on the expression of MMP9 and PTGS2 in cartilage tissue

MMP9 and PTGS2 are common molecules in the inflammatory pathway, and they are also the primary target proteins of JBJN in the treatment of KOA. Western blot data confirmed that the protein levels of cartilage MMP9 and PTGS2 in the tissue of the JBJN treatment group were significantly lower than those of the model control group (Figure 9).

Discussion

Traditional Chinese medicine formulas are developed based on TCM theories and individual conditions, combining a variety of herbs to form the appropriate drug structure for the treatment of various medical conditions.. This allows the drugs to produce synergistic and antagonistic effects and even generate new substances [14]. Network pharmacology of TCM compounds explores the potential mechanisms of TCM treatment and disease prevention by studying the complex chemical components and multi-target, multi-pathway mechanisms of Chinese herbal medicine [15]. The specific mechanism of JBJN in the treatment of KOA has not been thoroughly studied. Therefore, this study utilized network pharmacology to identify the active constituents, targets, and mechanisms of action responsible for JBJN's therapeutic effectiveness in treating KOA. Furthermore, the binding affinity between the key components of JBJN and target proteins was validated through molecular docking technology. Ultimately, animal

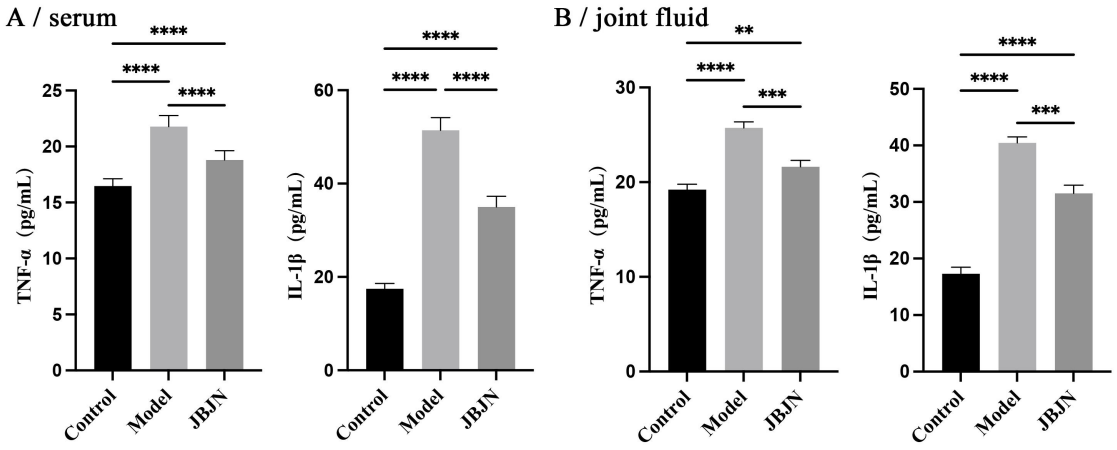

Figure 8 JBJN decreases the expression of inflammatory factors in KOA rats. (A) Quantitative analysis of TNF-α and IL-1β in serum ($\bar{x} \pm s$, $n = 8$). (B) Quantitative analysis of TNF-α and IL-1β in joint fluid ($\bar{x} \pm s$, $n=3$). One-way ANOVA (with Tukey's post-hoc test) was used for the statistical analysis. The significance levels were denoted as $^{**}P < 0.01$, $^{***}P < 0.001$, and $^{****}P < 0.0001$. JBJN, Juanbi capsule; KOA, knee osteoarthritis, ANOVA, analysis of variance; IL, interleukin; TNF, tumor necrosis factor.

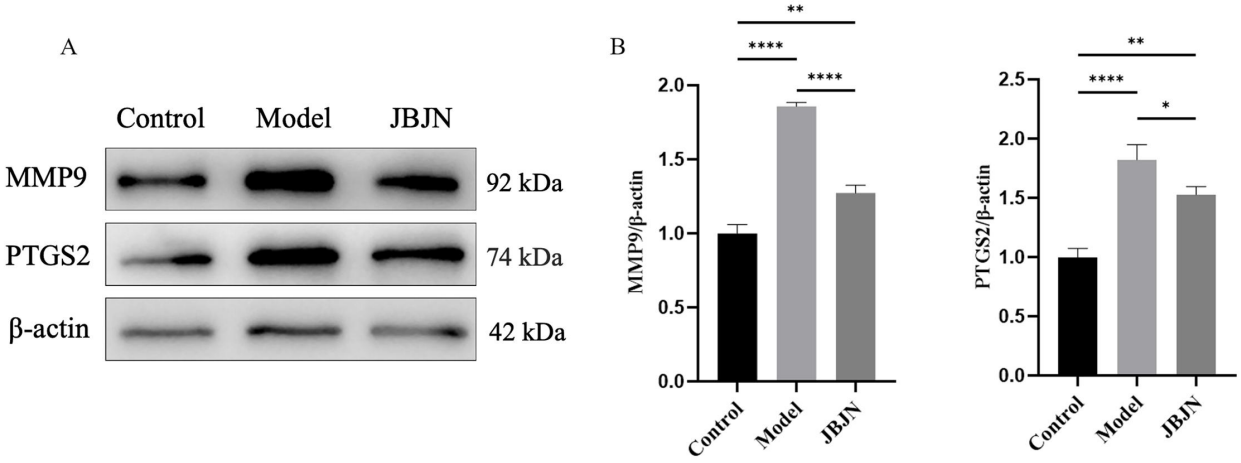

Figure 9 JBJN inhibits the expression of MMP9 and PTGS2 in cartilage tissue. (A) Representative western blotting figures of MMP9 and PTGS2. (B) Quantitative analysis of the protein expression levels of MMP9 and PTGS2 ($\bar{x} \pm s$, $n = 3$). One-way ANOVA (with Tukey's post-hoc test) was used for the statistical analysis. The significance levels were denoted as $^{*}P < 0.05$, $^{**}P < 0.01$, $^{***}P < 0.001$, and $^{****}P < 0.0001$. JBJN, Juanbi capsule; KOA, knee osteoarthritis, ANOVA, analysis of variance.

experiments were conducted to validate these findings and establish a theoretical basis for the clinical management of KOA.

The results of network pharmacology showed that quercetin, kaempferol, β-sitosterol, sitosterol, and luteolin may be the main components of JBJN in the treatment of KOA. In osteoarthritis, quercetin has good anti-inflammatory and cartilage-protective effects [16]. Quercetin has anti-inflammatory effects by inhibiting the NLRP3 signaling pathway, p38 activation, and endoplasmic reticulum stress, as well as inhibiting NO, TNF-α, and IL-1β [17, 18]. Qiu et al. discovered that quercetin can regulate ER stress-related chondrocyte apoptosis and facilitate the reversal of mitochondrial dysfunction in chondrocytes by activating the SIRT1/AMPK signaling pathway [19]. Hu et al. discovered that quercetin can regulate the polarization of synovial macrophages from M1 to M2, inhibit the inflammatory response of chondrocytes, and alleviate osteoarthritis in rats [20]. In addition to inhibiting inflammation, Permatasari et al. found that quercetin prevented proteoglycan destruction by inhibiting the expression of MMP3, MMP9, MMP13, and ADAMTS-5 in OA model rats [21]. Kaempferol has functions such as regulating inflammation and reducing oxidative stress. Zhuang et al. found that kaempferol could regulate IL-1β-induced inflammatory response in rat chondrocytes by inhibiting the expression of NF-κB signaling pathway [22]. Lee et al. found that kaempferol inhibited IL-1β-stimulated NF-κB ligand-receptor activator mediated osteoclastogenesis by down-regulating MAPKs, c-Fos, and NFATc1 [23]. Xiao et al. found that kaempferol could inhibit NF-κB activation and reduce inflammation by inhibiting the generation of reactive oxygen species and blocking the osteopontin related signaling pathway regulated by aldosterone [24]. Kaempferol can regulate the polarization of M1/M2 macrophages, and M1 macrophages have pro-inflammatory and accelerated cartilage destruction functions [25, 26]. β-sitosterol has anti-inflammatory, immunomodulatory, and analgesic effects [27]. Liao et al. found that β-sitosterol effectively inhibited the production of reactive oxygen species induced by lipopolysaccharide, inhibited the activation of NF-κB, and subsequently downregulated the expression of IL-6, IL-1β, and TNF-α in cells [28]. Stigmasterol can bind to the chondrocyte membrane and inhibit the expression of MMP and PTGS2 by inhibiting the NFκB pathway [29, 30]. Stigmasterol has the properties of reducing the expression of inflammatory factors and slowing down the catabolism of the cartilage matrix. Fei et al. discovered that luteolin can inhibit IL-1β-induced inflammation in rat chondrocytes, increase the production of type II collagen, and slow down the progression of osteoarthritis [31]. Through molecular docking analysis of key molecules and protein targets, it was found that quercetin, kaempferol, and β-sitosterol could target and regulate the expression of TNF-α, IL-1β, MMP9, PTGS2, TP53, VEGFA, and other proteins. This suggests that the active ingredients of JBJN have anti-inflammatory, antioxidant, immune-regulating, and cartilage matrix-protecting functions.

According to PPI network analysis, TNF, IL6, IL1β, MMP9, PTGS2, TP53, and VEGFA may be the critical targets of JBJN in the treatment of KOA. Studies have shown that the proinflammatory response induced by TNF-α, IL-1β, and IL-6 is closely related to M1 macrophages, which induces chondrocyte apoptosis and accelerated cartilage matrix degradation by leading to the production of pro-chondrocytic mediators [32, 33]. MMP9 is a component of the MMPs family, which can degrade most of the articular cartilage matrix, induce the apoptosis of articular chondrocytes, and eventually lead to severe destruction of knee cartilage. Studies have shown that MMP9 can promote the expression of inflammatory mediators such as TNF-α and IL-1β, aggravate local inflammation, destroy cartilage matrix, and cause subchondral bone microstructure disorder [34, 35]. PTGS2 is a prostaglandin-endoperoxide synthase, which is a potent mediator of inflammation and can promote the metabolism of arachidonic acid to prostaglandins and leukotrienes, which in turn leads to inflammation [36]. Celecoxib and other selective non-steroidal anti-inflammatory drugs as PTGS2 inhibitors have been widely used in the clinical treatment of KOA [37, 38]. Chondrocytes in patients with advanced osteoarthritis are highly expressed and promote new blood vessel formation, and VEGFA expression is gradually increased [39, 40]. VEGFA can upregulate the expression of MMPs in chondrocytes and downregulate the expression of extracellular matrix components, including aggrecan and type II collagen. TP53 is a tumor suppressor gene associated with tumorigenesis and a key signal that inhibits cell growth and promotes apoptosis. Studies have shown that KOA chondrocytes with high expression of p53 exhibit apoptotic or senescent morphology. Therefore, JBJN can interfere with the target proteins of KOA through a variety of classic inflammation, apoptosis, and cartilage metabolism processes and affect the development of KOA.

The results of the functional enrichment analysis revealed a significant enrichment of molecular proteins related to KOA in GO function and KEGG pathway. The biological process accounted for the largest proportion of GO analysis, and the content was mainly manifested in inflammatory response, cell migration regulation, reactive oxygen metabolism, hormone stress, cell proliferation, and others. The KEGG pathways were primarily enriched in the AGE-RAGE, IL-17, TNF, NF-κB, and PI3K-Akt signaling pathway. Among them, AGE is an advanced glycation end product, and RAGE is its receptor. During aging, AGE accumulates in articular cartilage and participates in the activation of proinflammatory responses and various inflammatory gene-related signaling pathways [41]. The AGE-RAGE signaling pathway can be activated downstream of chondrocytes NF-κB and MAPK signal pathway, stimulate endoplasmic reticulum stress, produce PTGS2 and NO cartilage cells, and induce inflammation of cartilage cells [42]. IL-17 signaling pathway and TNF signaling pathway, as classical inflammatory pathways, can activate NF-κB and MAPK signaling pathways, and induce synovial fibroblasts and chondrocytes to produce IL-1, Tnf-α, MMPs, and other chemokines [43]. NF-κB is a multifunctional transcription factor involved in a variety of biological processes and is associated with chondrocyte proliferation, apoptosis, and synovial inflammatory processes [44]. Studies have found that the NF-κB signaling pathway is abnormally activated in osteoarthritis, which directly or indirectly induces the expression of proinflammatory mediators such as MMP9, PTGS2, PGE2, and iNOS [45]. PI3K/AKT is a classical signaling pathway that regulates the autophagy response, which can maintain the homeostasis of chondrocytes, inhibit the apoptosis of chondrocytes, and promote the proliferation of chondrocytes, thereby slowing down the process of cartilage degeneration in KOA [46, 47].

In summary, the pathogenesis of KOA is complex, involving multiple interconnected signaling pathways that are cross-linked and mutually modulation. The active ingredients of JBJN can simultaneously modulate a variety of targets and pathways, showing the multi-component-multi-target-multi-pathway action pattern of TCM. Here, we utilized network pharmacology and molecular docking methods to investigate the mechanism of JBJN in treating KOA. And our investigation revealed that JBJN could decrease the levels of TNF-α and IL-1β in serum and synovial fluid of KOA rats, and downregulate the expression levels of MMP9 and PTGS2 proteins in the articular cartilage. However, our article does have some limitations. We did not conduct thorough experimental validation, and future studies should further validate the role of other pathways enriched in KEGG analysis, as well as the targets of different active ingredients of JBJN in KOA. In addition, the effective active ingredients of the drugs in this study were the values predicted by computer simulation, did not fully account for the changes in pharmacokinetics that occur after the active ingredients enter the body's metabolism. Therefore, further research is needed to understand the deeper molecular mechanisms.

References

1. Tang X, Wang S, Zhan S, et al. The Prevalence of Symptomatic Knee Osteoarthritis in China: Results From the China Health and Retirement Longitudinal Study. *Arthritis Rheumatol.*

2016;68(3):648–653. Available at: http://doi.org/10.1002/art.39465
2. Kim JR, Yoo J, Kim H. Therapeutics in Osteoarthritis Based on an Understanding of Its Molecular Pathogenesis. *Int J Mol Sci.* 2018;19(3):674. Available at: http://doi.org/10.3390/ijms19030674
3. Hunter DJ, Bierma-Zeinstra S. Osteoarthritis. *Lancet.* 2019;393(10182):1745–1759. Available at: http://doi.org/10.1016/S0140-6736(19)30417-9
4. Zhang W, Ouyang H, Dass CR, Xu J. Current research on pharmacologic and regenerative therapies for osteoarthritis. *Bone Res.* 2016;4(1):15040. Available at: http://doi.org/10.1038/boneres.2015.40
5. Yang M, Jiang L, Wang Q, Chen H, Xu G. Traditional Chinese medicine for knee osteoarthritis: An overview of systematic review. *PLoS One.* 2017;12(12):e0189884. Available at: https://doi.org/10.1371/journal.pone.0189884
6. Wang L, Zhang XF, Zhang X, et al. Evaluation of the Therapeutic Effect of Traditional Chinese Medicine on Osteoarthritis: A Systematic Review and Meta-Analysis. *Pain Res Manag.* 2020;2020:5712187. Available at: https://doi.org/10.1155/2020/5712187
7. Nevitt MC, Felson DT. Sex hormones and the risk of osteoarthritis in women: epidemiological evidence. *Ann Rheum Dis.* 1996;55(9):673–676. Available at: http://doi.org/10.1136/ard.55.9.673
8. Yuan P, Liu D, Chu X, Hao Y, Zhu C, Qu Q. Effects of Preventive Administration of Juanbi Capsules on TNF-α IL-1 And IL-6 Contents of Joint Fluid in the Rabbit with Knee Osteoarthritis. *J Tradit Chin Med.* 2010;30(4):254–258. Available at: http://doi.org/10.1016/S0254-6272(10)60052-0
9. Yuan P, Yu H, Zhou H, Zhu C, Qu Q, Liu D. Preventive Administration of Juanbi Capsules () for Knee Osteoarthritis: Effects on Serum MMP-2 and MMP-9 levels and Cartilage Repair. *J Tradit Chin Med.* 2011;31(4):334–337. Available at: http://doi.org/10.1016/S0254-6272(12)60014-4
10. Ru J, Li P, Wang J, et al. TCMSP: a database of systems pharmacology for drug discovery from herbal medicines. *J Cheminform.* 2014;6(1):13. Available at: http://doi.org/10.1186/1758-2946-6-13
11. Høegh-Andersen P, Tankó LB, Andersen TL, et al. Ovariectomized rats as a model of postmenopausal osteoarthritis: validation and application. *Arthritis Res Ther.* 2004;6(2):R169–R180. Available at: https://doi.org/10.1186/ar1152
12. Sniekers YH, Weinans H, Bierma-Zeinstra SM, van Leeuwen JPTM, van Osch GJVM. Animal models for osteoarthritis: the effect of ovariectomy and estrogen treatment–a systematic approach. *Osteoarthritis Cartilage.* 2008;16(5):533–541. Available at: http://doi.org/10.1016/j.joca.2008.01.002
13. Yang L, Xu H, Chen Y, et al. Melatonin: Multi-Target Mechanism Against Diminished Ovarian Reserve Based on Network Pharmacology. *Front Endocrinol* (*Lausanne*). 2021;12:630504. Available at: http://doi.org/10.3389/fendo.2021.630504
14. Fengtao P, Kesong LI, Yi Z, Xiaopo T, Xinyao Z. Efficacy of Lushi Runzao decoction on ameliorating Sjogren's syndrome: a networpharmacology and experimental verification-based study. *J Tradit Chin Med.* 2023;43(4):751–759. Available at: http://doi.org/10.19852/j.cnki.jtcm.2023.04.004
15. Jin J, Xu YY, Liu WP, Hu KH, Xue N, Zheng ZG. Simiao Wan alleviates obesity-associated insulin resistance via PKC ε /IRS-1/PI3K/Akt signaling pathway based on network pharmacology analysis and experimental validation. *Tradit Med Res.* 2023;8(10):60. Available at: http://doi.org/10.53388/TMR20230512002
16. Sirše M. Effect of Dietary Polyphenols on Osteoarthritis-Molecular Mechanisms. *Life* (*Basel*). 2022;12(3):436. Available at: https://doi.org/10.3390/life12030436
17. Li W, Wang Y, Tang Y, et al. Quercetin Alleviates Osteoarthritis Progression in Rats by Suppressing Inflammation and Apoptosis via Inhibition of IRAK1/NLRP3 Signaling. *J Inflamm Res.* 2021;Volume14:3393–3403. Available at: http://doi.org/10.2147/JIR.S311924
18. Wang XP, Xie WP, Bi YF, et al. Quercetin suppresses apoptosis of chondrocytes induced by IL-1β via inactivation of p38 MAPK signaling pathway. *Exp Ther Med.* 2021;21(5):468. Available at: http://doi.org/10.3892/etm.2021.9899
19. Qiu L, Luo Y, Chen X. Quercetin attenuates mitochondrial dysfunction and biogenesis via upregulated AMPK/SIRT1 signaling pathway in OA rats. *Biomed Pharmacother.* 2018;103:1585–1591. Available at: https://doi.org/10.1016/j.biopha.2018.05.003
20. Hu Y, Gui Z, Zhou Y, Xia L, Lin K, Xu Y. Quercetin alleviates rat osteoarthritis by inhibiting inflammation and apoptosis of chondrocytes, modulating synovial macrophages polarization to M2 macrophages. *Free Radical Biol Med.* 2019;145:146–160. Available at: http://doi.org/10.1016/j.freeradbiomed.2019.09.024
21. Bahtiar A, Permatasari D, Karliana D, Iskandarsyah I, Arsianti A. Quercetin prevent proteoglycan destruction by inhibits matrix metalloproteinase-9, matrix metalloproteinase-13, a disintegrin and metalloproteinase with thrombospondin motifs-5 expressions on osteoarthritis model rats. *J Adv Pharm Technol Res.* 2019;10(1):2–8. Available at: http://doi.org/10.4103/japtr.JAPTR_331_18
22. Zhuang Z, Ye G, Huang B. Kaempferol Alleviates the Interleukin-1β-Induced Inflammation in Rat Osteoarthritis Chondrocytes via Suppression of NF-κB. *Med Sci Monit.* 2017;23:3925–3931. Available at: http://doi.org/10.12659/MSM.902491
23. Lee WS, Lee EG, Sung MS, Yoo WH. Kaempferol Inhibits IL-1β-Stimulated, RANKL-mediated Osteoclastogenesis via Downregulation of MAPKs, c-Fos, and NFATc1. *Inflammation.* 2014;37(4):1221–1230. Available at: http://doi.org/10.1007/s10753-014-9849-6
24. Xiao HB, Lu XY, Liu ZK, Luo ZF. Kaempferol inhibits the production of ROS to modulate OPN–αvβ3 integrin pathway in HUVECs. *J Physiol Biochem.* 2016;72(2):303–313. Available at: http://doi.org/10.1007/s13105-016-0479-3
25. Li Y, Zheng D, Shen D, Zhang X, Zhao X, Liao H. Protective Effects of Two Safflower Derived Compounds, Kaempferol and Hydroxysafflor Yellow A, on Hyperglycaemic Stress-Induced Podocyte Apoptosis via Modulating of Macrophage M1/M2 Polarization. *J Immunol Res.* 2020;2020:2462039. Available at: http://doi.org/10.1155/2020/2462039
26. Xie J, Huang Z, Yu X, Zhou L, Pei F. Clinical implications of macrophage dysfunction in the development of osteoarthritis of the knee. *Cytokine Growth Factor Rev.* 2019;46:36–44. Available at: http://doi.org/10.1016/j.cytogfr.2019.03.004
27. Babu S, Jayaraman S. An update on β-sitosterol: A potential herbal nutraceutical for diabetic management. *Biomed Pharmacother.* 2020;131:110702. Available at: http://doi.org/10.1016/j.biopha.2020.110702
28. Liao PC, Lai MH, Hsu KP, et al. Identification of β-Sitosterol as in Vitro Anti-Inflammatory Constituent in Moringa oleifera. *J Agric Food Chem.* 2018;66(41):10748–10759. Available at: http://doi.org/10.1021/acs.jafc.8b04555
29. Gabay O, Sanchez C, Salvat C, et al. Stigmasterol: a phytosterol with potential anti-osteoarthritic properties. *Osteoarthritis Cartilage.* 2010;18(1):106–116. Available at: http://doi.org/10.1016/j.joca.2009.08.019
30. Chen WP, Yu C, Hu PF, Bao JP, Tang JL, Wu LD. Stigmasterol blocks cartilage degradation in rabbit model of osteoarthritis. *Acta Biochim Pol.* 2012;59(4):537–541. Available at:

http://doi.org/10.18388/abp.2012_2088
31. Fei J, Liang B, Jiang C, Ni H, Wang L. Luteolin inhibits IL-1β-induced inflammation in rat chondrocytes and attenuates osteoarthritis progression in a rat model. *Biomed Pharmacother.* 2019;109:1586–1592. Available at: http://doi.org/10.1016/j.biopha.2018.09.161
32. Hwang H, Kim H. Chondrocyte Apoptosis in the Pathogenesis of Osteoarthritis. *Int J Mol Sci.* 2015;16(11):26035–26054. Available at: http://doi.org/10.3390/ijms161125943
33. Wang L, He C. Nrf2-mediated anti-inflammatory polarization of macrophages as therapeutic targets for osteoarthritis. *Front Immunol.* 2022;13:967193. Available at: http://doi.org/10.3389/fimmu.2022.967193
34. Teng P, Liu Y, Dai Y, Zhang H, Liu WT, Hu J. Nicotine Attenuates Osteoarthritis Pain and Matrix Metalloproteinase-9 Expression via the α7 Nicotinic Acetylcholine Receptor. *J Immunol.* 2019;203(2):485–492. Available at: http://doi.org/10.4049/jimmunol.1801513
35. Jackson MT, Moradi B, Smith MM, Jackson CJ, Little CB. Activation of Matrix Metalloproteinases 2, 9, and 13 by Activated Protein C in Human Osteoarthritic Cartilage Chondrocytes. *Arthritis Rheumatol.* 2014;66(6):1525–1536. Available at: http://doi.org/10.1002/art.38401
36. Pang Y, Liu X, Zhao C, et al. LC－MS/MS-based arachidonic acid metabolomics in acute spinal cord injury reveals the upregulation of 5-LOX and COX-2 products. *Free Radical Biol Med.* 2022;193(Pt 1):363–372. Available at: http://doi.org/10.1016/j.freeradbiomed.2022.10.303
37. Puljak L, Marin A, Vrdoljak D, Markotic F, Utrobicic A, Tugwell P. Celecoxib for osteoarthritis. *Cochrane Database Syst Rev.* 2017;5(5):CD009865. Available at: http://doi.org/10.1002/14651858.CD009865.pub2
38. Sharma V, Bhatia P, Alam O, et al. Recent advancement in the discovery and development of COX-2 inhibitors: Insight into biological activities and SAR studies (2008–2019). *Bioorg Chem.* 2019;89:103007. Available at: http://doi.org/10.1016/j.bioorg.2019.103007
39. Chen W, Lin T, He Q, et al. Study on the potential active components and molecular mechanism of Xiao Huoluo Pills in the treatment of cartilage degeneration of knee osteoarthritis based on bioinformatics analysis and molecular docking technology. *J Orthop Surg Res.* 2021;16(1):460. Available at: http://doi.org/10.1186/s13018-021-02552-w
40. Hamilton JL, Nagao M, Levine BR, Chen D, Olsen BR, Im H. Targeting VEGF and Its Receptors for the Treatment of Osteoarthritis and Associated Pain. *J Bone Miner Res.* 2016;31(5):911–924. Available at: http://doi.org/10.1002/jbmr.2828
41. Hudson BI, Lippman ME. Targeting RAGE Signaling in Inflammatory Disease. *Annu Rev Med.* 2018;69(1):349–364. Available at: http://doi.org/10.1146/annurev-med-041316-085215
42. Nah SS, Choi IY, Lee CK, et al. Effects of advanced glycation end products on the expression of COX-2, PGE2 and NO in human osteoarthritic chondrocytes. *Rheumatology* (*Oxford*). 2008;47(4):425–431. Available at: http://doi.org/10.1093/rheumatology/kem376
43. Roman-Blas JA, Jimenez SA. NF-κB as a potential therapeutic target in osteoarthritis and rheumatoid arthritis. *Osteoarthritis Cartilage.* 2006;14(9):839–848. Available at: http://doi.org/10.1016/j.joca.2006.04.008
44. Gu R, Liu N, Luo S, Huang W, Zha Z, Yang J. MicroRNA-9 regulates the development of knee osteoarthritis through the NF-kappaB1 pathway in chondrocytes. *Medicine* (*Baltimore*). 2016;95(36):e4315. Available at: http://doi.org/10.1097/MD.0000000000004315
45. Choi, Jo, Park, Kang, Park. NF-B Signaling Pathways in Osteoarthritic Cartilage Destruction. *Cells.* 2019;8(7):734. Available at: http://doi.org/10.3390/cells8070734
46. Zhong JT, Yu J, Wang HJ, et al. Effects of endoplasmic reticulum stress on the autophagy, apoptosis, and chemotherapy resistance of human breast cancer cells by regulating the PI3K/AKT/mTOR signaling pathway. *Tumour Biol.* 2017;39(5):101042831769756. Available at: http://doi.org/10.1177/1010428317697562
47. Sun K, Luo J, Guo J, Yao X, Jing X, Guo F. The PI3K/AKT/mTOR signaling pathway in osteoarthritis: a narrative review. *Osteoarthritis Cartilage.* 2020;28(4):400–409. Available at: http://doi.org/10.1016/j.joca.2020.02.027